ISSN: 2621-4709 E-ISSN: 2621-2528
Journal of Applied Agricultural Science and Technology
Vol. 9 No. 2 (2025): 156-171

Thermal Properties and Cooling Simulation of Red Dragon Fruit Using the Finite Difference Method

Lailatul Maghfiroh [1,*], Sumardi Hadi Sumarlan [1], Hammam [1]

[1] Department of Biosystems Engineering, Universitas Brawijaya, Malang, Indonesia

Abstract. *Red dragon fruit (Hylocereus polyrhizus) can be transformed into various processed products, such as chips, jam, and juice. However, thermal processing may significantly alter its physical and chemical properties. As the calorific properties vary among different fruits, this study aims to measure the thermal properties of red dragon fruit. By measuring its thermal properties, red dragon fruit can be processed with improved energy efficiency and optimized thermal management. This study aims to examine the thermal properties and perform a cooling simulation of red dragon fruit. The cooling simulation, based on one-dimensional radial thermal flow, was conducted using the spherical heat equation explicitly discretized by the Forward Time Central Space (FTCS) scheme within the Finite Difference Method (FDM). The specific heat, thermal diffusivity, and thermal conductivity of red dragon fruit were 3.827 kJ/kg ^oC, 9.18 x 10^{-4} cm^2/s, and 0.34 W/m ^oC, respectively. The overall average coefficient of determination (R^2) from the validation test of the simulation results was 0.9654. Based on these findings, the one-dimensional (radial) discretized heat transfer equation model can be used to predict the temperature distribution in spherical fruit over time, based on its thermal diffusivity. However, this approach has limitations. Future research would benefit from measuring the thermal diffusivity of whole red dragon fruit and applying a three-dimensional discretized heat transfer equation to obtain more accurate results and minimize potential errors.*

Keywords: *cooling simulation; finite difference method; red dragon fruit; thermal properties.*

Type of the Paper: Regular Article

1. Introduction

Horticultural products possess properties that are highly susceptible to thermal influences [1]. Excessive thermal exposure may damage certain physical and chemical characteristics, which vary between different types of fruit. Each type of fruit exhibits different thermal properties at varying levels of maturity [2]. These thermal properties are influenced by the fruit's chemical composition [3].

Red dragon fruit (*Hylocereus polyrhizus*) contains various chemical components, including a high water content (84-90%), fat (0.887%), ash (0.706%), dietary fiber (1.108%), total sugar (5.60%), starch (0.364%), and carbohydrates (5.97%) [4]. This high water content in red dragon fruit makes it more susceptible to damage when stored for extended periods at room temperature or during the distribution. This vulnerability also applies when the fruit is stored under refrigeration. When stored in a cooling environment, dragon fruit undergoes changes in its physical

https://doi.org/10.55043/jaast.v9i2.317
Received July 12, 2024; Received in revised form April 16, 2025; Accepted April 27, 2025; Published May 25, 2025
* First corresponding author
Email: maghfirohlailatul32@gmail.com
© 2024 The Authors. Published by Green Engineering Society on Journal of Applied Agricultural Science and Technology
This is an open access article under the CC BY-SA 4.0 license https://creativecommons.org/licenses/by-sa/4.0

structure, becoming more wilted and softer, with reduced chemical content, flavor, and freshness [5]. Dragon fruit stored in a cooling environment for two weeks at a room temperature of 20°C shows browning of the outer layer and darkening of the tendrils [6]. Prolonged cooling can also lead to biological damage due to water evaporation during storage in refrigeration [7].

Given these issues, it is essential to determine the values of thermal properties—such as specific heat, diffusivity, and thermal conductivity—before conducting post-harvest processing that involves temperature. Specific heat is the amount of heat or heat energy required to change the temperature of a material with a mass of 1 kg (or 1 g) by 1°C. In simpler terms, specific heat refers to a material's ability to absorb or release heat [8]. The higher the specific heat of a material, the greater the amount of heat energy required to increase its temperature. Thermal diffusivity refers to the rate at which temperature distributes through a material [9]. A higher thermal diffusivity value results in faster temperature changes within the product. Heat diffusivity is inversely proportional to specific heat and density, but directly proportional to thermal conductivity [10]. Meanwhile, thermal conductivity is a constant property of a material that indicates its ability to conduct heat [11]. Therefore, based on these data, the rate of temperature distribution can be determined, allowing the simulation of temperature change in the fruit and enabling more efficient thermal processing.

Calculations of thermal properties such as specific heat, thermal diffusivity, and thermal conductivity were conducted by Hawa et al. [12], using puyang chili as the test material. Specific heat was determined through calculations based on water content, thermal diffusivity was obtained using the finite difference method by solving the Crank–Nicolson scheme with one-dimensional heat flow in a tube, and thermal conductivity was calculated using a standard computational method. The results showed that the specific heat values for green, orange, and red puyang chilies were 2.992 ± 0.00, 3,100 ± 0.01, and 3.133 ± 0.01 kJ/kg°C, respectively. The corresponding thermal diffusivity values were $7.71 \times 10^{-8} \pm 5.06 \times 10^{-9}$, $9.16 \times 10^{-8} \pm 1.13 \times 10^{-9}$, and $1.01 \times 10^{-7} \pm 7.11 \times 10^{-9}$ m^2/s. Meanwhile, the thermal conductivity values for green, orange and red chilies were 0.241 ± 0.016, 0.298 ± 0.005, and 0.344 ± 0.025 W/m°C, respectively. However, determining specific heat based solely on water content is less accurate; therefore, it is necessary to incorporate other chemical components in the calculation to improve measurement accuracy. The thermal diffusivity value for one-dimensional flow can also be determined using the finite difference method with an explicit scheme, as demonstrated by Nurullaeli [13].

Once the thermal properties are known, temperature changes within the material can be accurately simulated. Temperature changes simulations have been conducted by Emmilia [14], who performed a cooling simulation on whole avocados by assuming the fruit to be spherical in shape. Accordingly, the spherical heat equation was used and solved using the finite difference

method with an explicit FTCS (Forward Time and Central Space) scheme, considering a one-dimensional (radial) heat source. Based on the comparison between observed and simulated temperatures, the coefficient of determination (R^2) ranged from 0.91 to 0.97. However, the simulation in this study was conducted using Delphi 7 software and only produced numerical temperature data, making it impossible to visually represent the temperature distribution within the fruit.

A study by Noor et al. [15] also investigated the simulation of temperature distribution in thin zinc and platinum plates using the finite difference method with the explicit FTCS (Forward Time and Central Space) scheme. The simulation was conducted using MATLAB software. In this study, the temperature distribution was presented visually, revealing a difference in the central temperature of the two materials, with a variation of approximately ±7.69°C. This difference was attributed to the distinct thermal conductivities of zinc and platinum.

Building on previous research, this study determined the thermal properties of red dragon fruit, specifically the specific heat, by analyzing the chemical composition, including carbohydrates, fat, protein, ash, and water content. The thermal diffusivity was determined using 1D cold thermal flow and calculated via the explicitly derived diffusion equation FTCS (Forward Time and Central Space) with the finite difference method. Thermal conductivity was determined using a separate calculation method. Experimental data on temperature changes during cooling simulations were obtained using whole red dragon fruit. The aim of this research was to examine the thermal properties (specific heat (cp), thermal diffusivity (α), and thermal conductivity (k)) as well as to conduct a cooling simulation on red dragon fruit using the derived spherical conduction equation, which was solved using the explicit finite difference scheme (FTCS) method, assuming one-dimensional (radial) heat flow.

2. Materials and Methods

2.1. Research Tools and Materials

The equipment used in this research included a cooling machine (LG refrigerator), a cooling chamber isolator for diffusivity experiments, a K-type stainless steel thermocouple, an Arduino Mega 2560 R3 CH340 microcontroller, a 1 kg Digi Pounds scale, a Memmert oven (model UN55), a B-ONE Ceramic Fiber Muffle Furnace, a 250 ml Soxhlet Extractor (Pyrex), distillation equipment (KjelMaster K-375), digestion equipment (Kjelsampler digester K-376), ArduinoIDE software, MATLAB R2022a (v9.12.0). The materials used in this research were red dragon fruit (*Hylocereus polyrhizus*) obtained from dragon fruit farmers, approximately 7-8 weeks old after the flower buds had formed. The fruit exhibited bright red skin and a slightly soft texture when squeezed. We further selected fruits based on similar diameters, specifically around 10 cm.

Additional materials included ice cubes, salt, and aluminum foil.

2.2. Research Design

The circuit design for measuring temperature distribution to determine the thermal diffusivity value of red dragon fruit requires several components. These include an insulating container (styrofoam) with a horizontal pipe tube (D = 2.5 cm, L = 10 cm), a cooling machine, a type K thermocouple temperature sensor, an Arduino Mega microcontroller, and a computer. The thermal diffusivity measurement must be conducted in a fixed, closed setup, with heat flow directed in one dimension. First, a perforated plastic tube (pp) is used, with five perforations, as shown in Fig. 1. The tube is then pressed firmly against one side of the dragon fruit until it penetrates through to the other end. Both ends of the tube are sealed with aluminum foil, each fitted with a thermocouple. The tube is then wrapped with a 4 cm thick removable styrofoam sleeve, also fitted with a thermocouple aligned with the five perforations. Next, the pipe is inserted into the cooling chamber insulation, and a thermocouple is connected. Finally, ice cubes are placed at both ends of the pipe during the temperature measurement process. The temperature was maintained at 0°C. The circuit was then placed in a cooling machine to prevent rapid melting of the ice. Temperature distribution was observed at five points, with measurements taken every second up to 9000 seconds. The sequence for collecting temperature distribution data to measure thermal diffusivity is shown in Fig. 1.

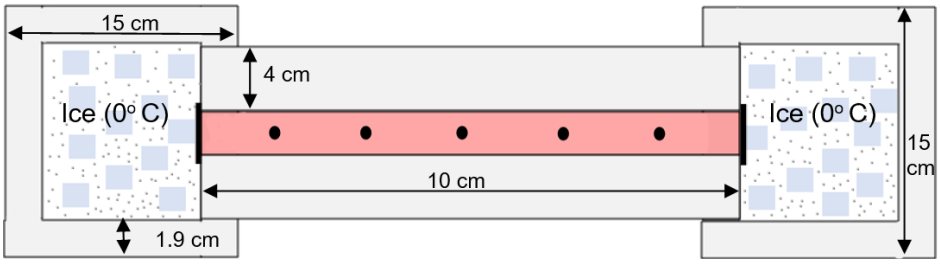

Fig. 1. Series of temperature distribution measurements for thermal diffusivity

To measure the temperature distribution, experiments were conducted on whole dragon fruits, which were wrapped in aluminum foil to allow direct heat conduction from the thermal source. A thermocouple was then inserted into the fruit at various depths, starting from the center and spaced 1 cm apart. In the process, the dragon fruit was placed in an insulated room containing ice and salt, with the temperature maintained at 0°C. The cooling chamber circuit was then inserted into the cooling machine. Temperature distribution was monitored at intervals of 1 second to 12,000 seconds. The series of temperature distribution data collected during the experiment is shown in Fig. 2.

Then, the specific heat value was determined using an equation based on the chemical composition (carbohydrates, fat, protein, ash content, and water content) and the thermal conductivity was calculated using a method based on the specific heat value, thermal diffusivity,

and density of the red dragon fruit.

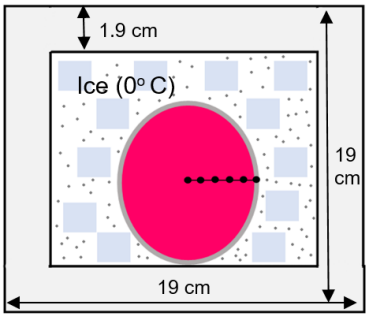

Fig. 2. Temperature distribution measurement network for the experiment

2.3. Analysis Method

The fat percentage was determined using the soxhletation method, referring to SNI 01-2891-1992 Point 8 [16], which required 2 grams of solid dragon fruit samples. The sample was hydrolyzed with 25% hydrochloric acid to free the bound fat, using a ratio of 30 ml of 25% HCl, 20 ml of distilled water, and sufficient boiling stones, and then boiled for 15 minutes under reflux. The mixture was then filtered using pre-weighed filter paper. Subsequently, the sample and filter paper were washed with hot distilled water. The filter paper containing the sample was dried at 100 - 105°C to evaporate residual moisture. Afterwards, the dried filter paper with the sample was placed in a soxhlet apparatus, and fat was extracted using alcohol at a temperature of 80°C for approximately 6 hours with a minimum of two cycles. The fat flask containing the extracted fat was then dried at 100-105°C to evaporate the solvent [17]. The fat content was calculated using Eq. (1) [18].

$$\%Fat\ content = \frac{(C-A)}{B}\ x\ 100\ \% \quad (1)$$

Where A is the weight of the empty fat flask (g), B is the weight of the test portion (g), and C is the fixed weight of the fat flask + test portion after heating (g).

Determination of total protein in food is generally carried out using the Kjeldahl method [19], in which the protein content was measured by weighing 1 gram of the sample and placing it in a 300 mL Kjeldahl tube. Then, 1 g of selenium and 12 mL of concentrated H_2SO_4 were added. The kjelDigester was preheated to 420°C. The 300 mL kjehdal tube was inserted into the KjelDigester, and the scrubber unit was activated to digest protein at 420°C for one hour. After digestion, the tube was removed and allowed to cool to room temperature. The kjehdahl tube was then installed in the distillation apparatus, followed by the addition of approximately 50 mL of distilled water and 50 mL of 40% NaOH. A 250 mL Erlenmeyer flask containing 25 mL of 4% H_3BO_3 was placed as a reservoir for the distillation unit. Distillation of the sample was carried out until the distillate volume reached at least 3x the volume of the initial reservoir. During the distillation process, the color of the container changed from red to green. The distillate was then

titrated with 0.2 N HCl solution until the endpoint changed from green to red. A blank solution was processed during each digestion cycle. The calculation of protein content, based on SNI 01-2891-1992 Point 7.1, was conducted using Eq. (2) [16,20].

$$\%Protein\ content = \frac{(V_p - V_b)x\ N\ x\ 1.4007\ x\ Fk}{W} \quad (2)$$

Where V_p is the volume of 0.2 N HCl required for sample titration (mL), V_b is the volume of 0.2 N HCl required for blank titration (mL), N is the normality of the 0.2 N HCl solution, Fk is the protein conversion factor, and W is the sample weight (g) or sample volume (mL). The protein conversion factor used in this research is 6.25.

Then the ash content was determined based on SNI 01-2891-1992 point 6.1 [16], in which 2-6 grams of the test portion sample was placed in a pre-weighed porcelain cup. The sample was then heated until the smoke disappeared. After that, ashing was performed in a furnace at 550°C for approximately 4 hours. The sample was then cooled in a desiccator, and its fixed weight was measured. The calculation of ash content was carried out using Eq. (3) [16,21].

$$\%Ash\ content = \frac{(C-A)}{B}\ x\ 100\% \quad (3)$$

Where A is the weight of the empty cup (g), B is the weight of the test portion (sample) (g), and C is the fixed weight of the fat flask plus test portion after boiling (g).

Water content was determined using the gravimetric method by evaporating moisture from the sample in an oven [22]. It was calculated based on the ratio of water weight to total weight. The sample was dried at 105°C. The equation used for finding water content is given in Eq. (4) [21–23].

$$\%\ \text{Water content} = \frac{w1}{w2}\ x\ 100\% \quad (4)$$

Where w_1 is the mass of water (g) (the total mass minus the dry mass of material), and w_2 is the total mass of material (g).

Determination of the carbohydrate percentage was carried out based on the Food and Drug Supervisory Agency reference [24], where the total carbohydrate content was calculated as percentage of the total sample minus the percentages of other chemical contents. The equation for determining carbohydrates content (%) is given in Eq. (5) [25,26].

$$\%Carbohydrates = 100\% - (\%protein\ +\ \%\text{fat} +\ \%\text{ash} +\ \%\text{water}) \quad (5)$$

Density was determined based on the ratio of the mass to the volume of the material. In this research, the mass of dragon fruit was weighed, and its volume was measured by placing the fruit in a measuring container filled with water. The displaced water was recorded as the volume of the dragon fruit. The density of dragon fruit was calculated as the ratio of its mass to volume, as shown in Eq. (6) [27,28].

$$\rho = \frac{m_{sample}}{V_{sample}} \quad (6)$$

Where ρ is the density of the material (kg/m^3), m_{sample} is the mass of the sample (kg), and V_{sample} is the volume of the sample (m^3).

Specific heat can be determined using Eq. (7) [29].

$$Cp = 1.424\,Xh + 1.549\,Xp + 1.675\,Xf + 0.837\,Xa + 4.187\,Xw \quad (7)$$

Where Cp is the specific heat (kJ/kg ^{o}C), Xh is the proportion of carbohydrate content in the material (%), Xp is the proportion of protein content in the material (%), Xf is the proportion of fat content in the material (%), Xa is the proportion of ash content in ingredients (%), and Xw is the proportion of protein content in ingredients (%).

The thermal diffusivity value in this study was determined based on the diffusion equation, which was solved using the finite difference method. The diffusion equation used is presented in Eq. (8,9) [30].

$$\frac{\partial T}{\partial t} = \mathrm{D}\,\frac{\partial^2 T}{\partial \mathrm{x}^2} \quad (8)$$

$$\mathrm{D} = \alpha\,\frac{\Delta t}{\Delta \mathrm{x}^2} \quad (9)$$

The equation was then solved using the finite difference method with the explicit FTCS (Forward Time Central Space) scheme to determine the thermal diffusivity value at a certain point and time, as shown in like Eq. (10,11,12,13) [14,15].

$$\frac{\partial T}{\partial t} = \frac{T_i^{j+1} - T_i^j}{\Delta t} \quad (10)$$

$$\frac{\partial^2 T}{\partial x^2} = \frac{T_{i-1}^j - 2T_i^j + T_{i+1}^j}{\Delta x^2} \quad (11)$$

$$\frac{\partial T_i^{j+1}}{\partial t} = \alpha\,\frac{\partial^2 T_i^{j+1}}{\partial x^2} \quad (12)$$

$$\alpha = \frac{(\Delta x)^2}{\Delta t}\left[\frac{T_i^{j+1} - T_i^j}{T_{i-1}^j - 2T_i^j + T_{i+1}^j}\right] \quad (13)$$

Where i is the grid of measurement points (cm), j is the grid of measurement times (s), Δx is the distance between measurement points, and Δt is the time interval between measurements. The stability condition for the thermal diffusivity value was determined, namely the D value $\leq$0.5 [14].

The thermal conductivity value was then determined by calculating the product of the specific heat, density and thermal diffusivity values of the material, as shown in Eq. (14) [31,32].

$$k = cp\,.\,\rho\,.\,\alpha \quad (14)$$

Where cp is specific heat (J/kg ^{o}C), ρ is the density (kg/m^3), and α is thermal diffusivity (m^2/s). The thermal conductivity values can then be compared, as shown in Eq. (15) [33].

$$k = 0.25\,Xh + 0.155\,Xp + 0.16\,Xf + 0.135\,Xa + 0.58\,Xw \quad (15)$$

The simulation of temperature changes (cooling) was determined using the spherical heat

conduction equation. The general form of the heat conduction equation in a sphere is given in Eq. (16) [34].

$$\frac{1}{r}\frac{\partial^2}{\partial r^2}(rT) + \frac{1}{r^2 sin\theta}\frac{\partial}{\partial \theta}\left(sin\theta\frac{\partial T}{\partial \theta}\right) + \frac{1}{r^2 sin^2\theta}\frac{\partial^2 T}{\partial \emptyset^2} + \frac{q}{k} = \frac{1}{\alpha}\frac{\partial T}{\partial t} \quad (16)$$

However, in this study, it is assumed that heat distribution only occurs in the radial direction (1D) and is not influenced by the Ø angle or Θ angle. Therefore, the heat equation used is given in Eq. (17) [34].

$$\frac{\partial T}{\partial t} = \alpha\left(\frac{\partial^2 T}{\partial r^2} + \frac{2}{r}\frac{\partial T}{\partial r}\right) \quad (17)$$

The above equation can be solved using a partial derivative finite difference equation with the FTCS (Forward Time Central Space) scheme. The resulting derivative for T(r,t) is given in Eq. (18,19) [34].

$$\left(\frac{T_{ri}^{tk+\Delta t} + T_{ri}^{tk}}{\Delta t}\right) = \alpha\left(\left(\frac{T_{ri-\Delta r}^{tk} - 2T_{ri}^{tk} + T_{ri+\Delta r}^{tk}}{\Delta r^2}\right) + \left(\frac{2}{ri}\right)\left(\frac{T_{ri+\Delta r}^{tk} + T_{ri-\Delta r}^{tk}}{2 * \Delta r}\right)\right) \quad (18)$$

$$T_{ri}^{tk+\Delta t} + T_{ri}^{tk} = \quad (19)$$
$$\left(\left(\frac{\alpha * \Delta t}{\Delta r^2}\right)\left(T_{ri-\Delta r}^{tk} - 2T_{ri}^{tk} + T_{ri+\Delta r}^{tk}\right) + \left(\frac{\alpha * \Delta t}{2 * \Delta r}\ x\ \frac{2}{ri}\right)\left(T_{ri+\Delta r}^{tk} + T_{ri-\Delta r}^{tk}\right)\right)$$

In equation (19), $\left(\frac{\alpha*\Delta t}{\Delta r^2}\right)$ (D) represents the diffusion constant, which has a stability requirement of D ≤ 0.5. For brevity, the diffusion constant $\left(\frac{\alpha*\Delta t}{\Delta r^2}\right)$ can be written as D and D1 for $\left(\frac{\alpha*\Delta t}{2*\Delta r^2}\right)$. The equation used is given in Eq. (20) [34].

$$T_{ri}^{tk+\Delta t} = T_{ri}^{tk} +$$
$$\left(D * \left(T_{ri-\Delta r}^{tk} - 2T_{ri}^{tk} + T_{ri+\Delta r}^{tk}\right) + \left(D1\ x\ \frac{2}{ri}\right)\left(T_{ri+\Delta r}^{tk} + T_{ri-\Delta r}^{tk}\right)\right) \quad (20)$$

Since the program uses the MATLAB application to display temperature distribution images in circular (polar) form, the Ø angle is needed to create a circular pattern. The polar coordinates are then converted to Cartesian coordinates using the pol2cart command. The equations for the simulation used in the MATLAB program are given in Eq. (21) [34].

$$T_{ri,\emptyset j}^{tk+\Delta t} = T_{ri,\emptyset j}^{tk} +$$
$$\left(D * \left(T_{ri-\Delta r,\emptyset j}^{tk} - 2T_{ri,\emptyset j}^{tk} + T_{ri+\Delta r,\emptyset j}^{tk}\right) + \left(D1\ x\ \frac{2}{ri}\right)\left(T_{ri+\Delta r,\emptyset j}^{tk} + T_{ri-\Delta r,\emptyset j}^{tk}\right)\right) \quad (21)$$

From equation (21), when T (ri, Øj, tk) = Ti,j,k the equation can be discretized as shown in Eq. (22) [34].

$$T_{i,j}^{k+1} = T_{i,j}^{k} + \left(D * \left(T_{i-1,j}^{k} - 2T_{i,j}^{k} + T_{i+1,j}^{k}\right) + \left(D1\ x\ \frac{2}{ri}\right)\left(T_{i+1,j}^{k} + T_{i-1,j}^{k}\right)\right) \quad (22)$$

The parameters entered into the MATLAB software to simulate temperature changes include

the thermal diffusivity value, inner radius (r_in) = 0 cm, outer radius (r_out) = 5 cm, number of segments (m) = 5, between nodes (delta_r) = 1 cm, number of nodes (nr) = 6, total angle (nphi) = 36, total time (t) = 12000 s, and time difference (delta_t) = 1 s. The boundary conditions used are as follows:

Initial Condition: T(r,t =0) = Tin = 28^{o}C

Boundary Condition: at r = r_out, T (5,t) = Trout = 0^{o}C (Dirichlet BC)

The output data displayed in the MATLAB software showed the temperature distribution from the simulation results. The output represented the temperature change occurring radially every 1 s for 12000 s. The simulation results were compared with experimental data using R^2 regression.

3. Results and Discussion

3.1. Specific Heat

Based on the chemical composition of red dragon fruit, the carbohydrate percentage was 11.06%, fat was 0.59%, protein was 0.43%, ash content was 0.85% and water content was 87%. From these values, the specific heat was 3.827 kJ/kg^{o}C. This specific heat value aligns with the results of Rofi'ah [35], who reported 3.507 - 3.796 kJ/kg^{o}C for red dragon fruit. When compared to the data from Bhagya Raj et al. [36], which reported a specific heat of 3.350 kJ/kg^{o}C, the value obtained in this study is slightly higher.

The variation in the specific heat value of red dragon fruit can be influenced by its chemical composition. Different stages of maturity result in distinct chemical composition values. Fruit left too long after harvest exhibit a decrease in water content, as indicated by weight loss and wrinkling due to evapotranspiration, which also affects the specific heat value. The specific heat influences the amount of heat energy required: the higher the specific heat, the higher the energy required to increase the temperature.

3.2. Thermal Diffusivity

The average thermal diffusivity of red dragon fruit determined in this study was 9.18 x 10-4 cm^2/s. A higher thermal diffusivity value indicates faster temperature propagation within the fruit. In this study, with a data collection interval of 1 s, the thermal diffusivity fluctuated from the beginning to the end of the cooling process. However, increasing the data collection interval Δt decreases precision and accuracy, as the stability requirement for thermal diffusivity is a diffusion coefficient (D) $\leq$ 0.5.

A similar observation was made in the study by Karneta et al. [37], where the thermal diffusivity of pempek lenjer during boiling fluctuated but was generally higher at the beginning of the heating process. These fluctuations in thermal diffusivity were influenced by temperature measurements, as voltage fluctuations also occurred during temperature data collection. Such

fluctuations can arise from several sources, including jumper connections on the Arduino Mega, PCB, or solder connections. Additionally, power supply drops in the Arduino Mega circuit may alter the retention for the ADC (Analog Digital Conversion) process.

Other factors influencing the thermal diffusivity of red dragon fruit include the fruit's structure, chemical composition, and physical characteristics. In this case, the most visible factors contributing to resistance are the specific heat and density values, with the specific heat being further influenced by the material's chemical composition.

Based on the results of testing the chemical composition of red dragon fruit, the largest water content was 87%. According to Kumar et al. [38], higher water content in fruit results in greater thermal diffusivity values, as water is an effective heat conductor. During the cooling process, the water content in dragon fruit decreases, which can lead to a denser fruit structure and fluctuating thermal diffusivity values until the end of the cooling process [39]. Variations in compositions affect heat transferred in the material, significantly influencing the resulting thermal diffusivity value.

Another chemical factor that influences and impedes thermal diffusivity is fat, which has insulating properties against transmitted heat. As reported by Zain et al. [40] in a study on the application and function of porang in frozen yogurt, fat can stabilize the air cavity in the ice cream structure, preventing it from melting easily due to a slower thermal diffusivity rate. The presence of fat and protein during heating can form surface deposits that hinder temperature distribution. The proximate content of ingredients such as carbohydrates, fats and proteins, can obstruct heat diffusion, thereby reducing the rate of temperature distribution in the product.

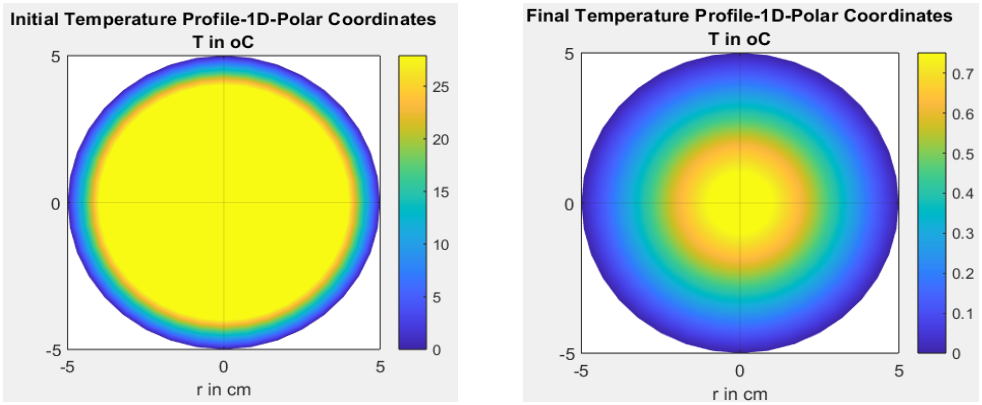

(a) (b)

Fig. 3. Simulation of temperature distribution at: (a) time 0 s and (b) time 12000 s

3.3. Thermal Conductivity

Thermal conductivity was determined based on the values of cp, α, and ρ. The ρ value obtained in this study was 973.45 kg/m^3. Based on the calculation method, the thermal conductivity of red dragon fruit in this study was 0.34 W/m^{o}C. In comparison, the thermal conductivity calculated using chemical composition was 0.53 W/m^{o}C. The thermal diffusivity values produced

in this study tended to be lower than expected. This may be due to temperature reading fluctuations caused by voltage instability, resulting in thermal diffusivity values that are either lower or higher than the actual values.

When compared with the results from research conducted by Bhagya Raj et al. [36], the thermal conductivity of red dragon fruit was 0.48 W/m ºC. The results also show notable differences. Factors influencing this, in addition to thermal diffusivity, include the specific heat value and the density value of the dragon fruit. Specific heat is influenced by several chemical compositions such as carbohydrates, fats, proteins, ash content, and water content [41]. At different levels of ripeness, the proportion of these chemical components vary. Density also affects heat conduction in dragon fruit. The greater the specific heat and density values, the greater the thermal conductivity [42].

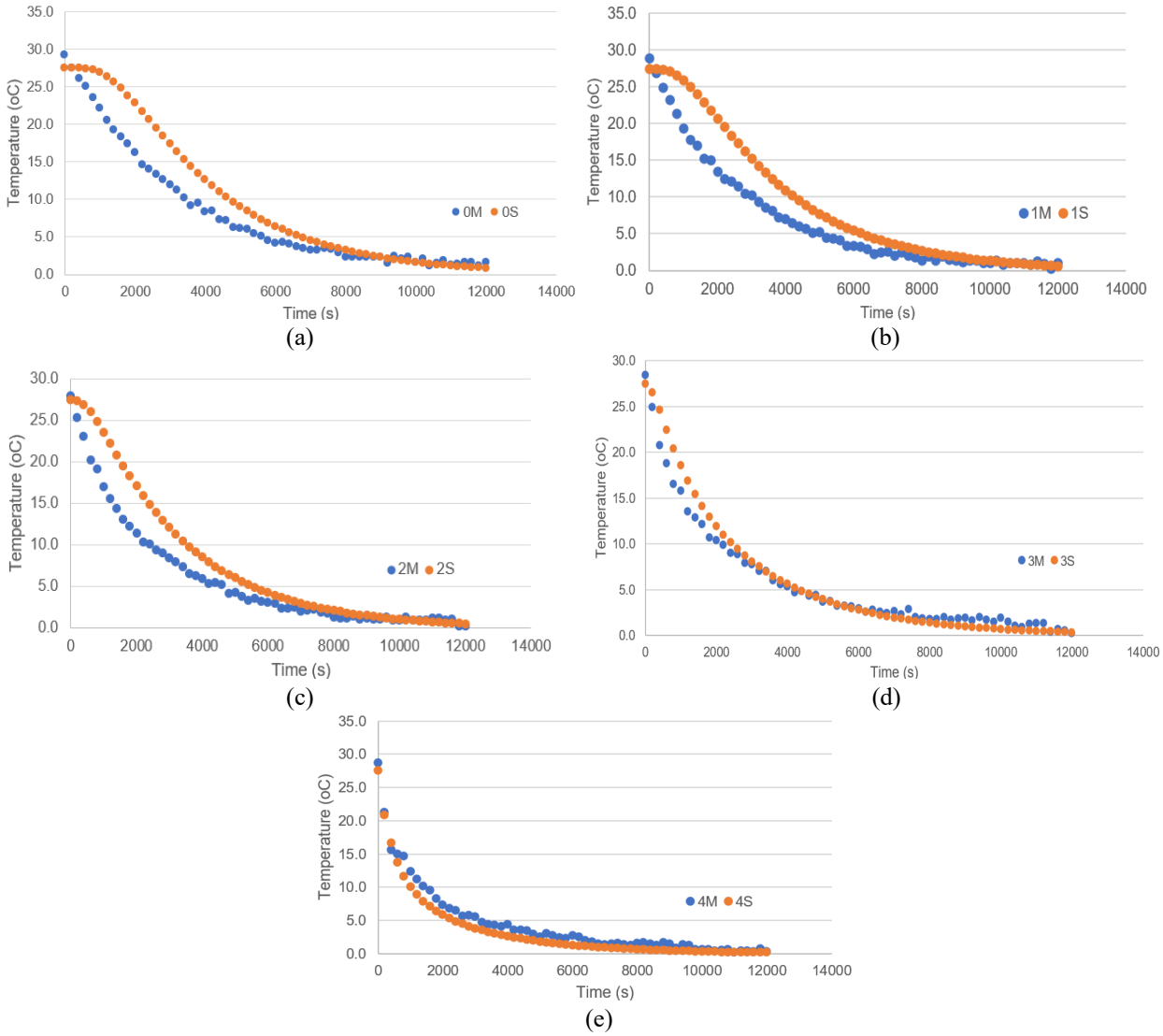

Fig. 4. Comparison of measured (M) and simulation (S) temperatures at distances: (a) 0 cm, (b) 1 cm, (c) 2 cm, (d) 3 cm, and (e) 4 cm

3.4. Simulation of Temperature Distribution Using MATLAB R2022a apk

The simulation results of temperature changes in this research can be seen in Fig. 3. The

initial condition before the temperature distribution was characterized by the inside of the dragon fruit appearing yellow, indicating an initial temperature of 28°C, while the outside (Trout) was 0°C, marked in blue. Each color represents the temperature distribution becoming lower towards the center, indicating the temperature changes were approaching the thermal source. The deeper the temperature distribution, the slower the change. Therefore, in the central part, the temperature decreases much slower than in other parts. This is in accordance with Sulistyaningtyas et al. [43], who stated that the slowing of temperature distribution is influenced by the size of the cross-sectional area.

3.5. Validation of Measurement Results (Experiment) and Simulation

The measured temperature data were compared with the simulation results using the R^2 value. A comparison of the measurement and simulation results is presented in Fig. 4.

Based on validation of the measurement results with the simulation, the R^2 value at 0 cm from the center was 0.9488 with a standard error of 1.77. At 1 cm from the center, the R^2 value was 0.9468 with a standard error of 1.71. At 2 cm, the R^2 value was 0.9623 with a standard error of 1.31, while at 3 it was 0.9844 with a standard error of 0.77. At 4 cm from the center, the R^2 value was 0.9851 with a standard error of 0.67. The overall average R^2 value was 0.9654. Based on the validation results, significant differences were observed in Fig. 4 a-c, which may be attributed to the uneven thickness of the red dragon fruit skin and on the other hand. Additionally, the major influencing factor is the thermal diffusivity estimation approach, which was based on an explicitly discretized 1D heat transfer equation. In practice, thermal diffusivity should be measured in a closed system; however, this study relied on the assumption that heat flow occurs only in 1D. Furthermore, if the radius is increased, there is a possibility that differences in the temperature trend may occur, which could also lead to variations in the average R^2 value. However, if the average R^2 value remains above 0.95, the results can still be considered satisfactory. Although the present study on cooling simulation using 1D radial thermal flow—modeled via the spherical heat conduction equation and explicitly discretized using the Forward Time Central Space (FTCS) scheme of the Finite Difference Method—has not been specifically applied to red dragon fruit, a similar approach has been reported by Emmilia [14]. In her study, cooling simulations were conducted on whole avocados. Accordingly, the spherical heat conduction equation was applied and solved using the explicit scheme FTCS (Forward Time and Central Space) method, under the assumption that heat transfer occurs radially in 1D. Based on the results of the relationship between observed and simulated temperatures, the R^2 value ranged from 0.91 to 0.97, which is consistent with the findings in the present study. However, in Emmilia's research, Delphi 7 software was used, and the output was limited to numerical comparisons of temperature data. As a result, the temperature distribution across the fruit could not be visually illustrated.

Based on the results and limitations of this study, future research would benefit from measuring the thermal diffusivity of whole red dragon fruit using a 3D discretized heat transfer equation. This approach could provide more accurate results and minimize potential errors. Nonetheless, the 1D radial discretized heat transfer equation model used in this study has been proven to be effective for observing temperature distribution in spherical-shaped fruit over a given period.

4. Conclusions

The specific heat, thermal diffusivity, and thermal conductivity values of red dragon fruit obtained in this study were 3.827 kJ/kg^{o}C, 9.18 x 10^{-4} cm^2 /s, and 0.34 W/m^{o}C, respectively. Based on the R^2 validation test, the simulation results of temperature changes were consistent with the experimental data, with the R^2 values of 0.9488 at 0 cm, 0.9468 at 1 cm, 0.9622 at 2 cm, 0.9844 at 3 cm, and 0.9851 at 4 cm from the center, yielding an average R^2 of 0.9654. The results indicate that the 1D (radial) discretized heat transfer equation model is suitable for simulating temperature distribution in spherical fruit over time based on its thermal diffusivity. However, limitations were observed in the validation results, particularly within 0-2 cm from the center, where significant discrepancies occurred. However, the average R^2 value obtained in this study was 0.9654, which is above 0.95, indicating that the results were still acceptable. Nevertheless, future research could benefit from measuring thermal diffusivity of whole red dragon fruit using a 3D discretized heat transfer equation to achieve more accurate results and minimize potential errors.

Abbreviations

FTCS forward time and central space
FDM finite difference method

Data availability statement

Data will be made available on request.

CRediT authorship contribution statement

Lailatul Maghfiroh: Conceptualization, Methodology, Software, Data Curation, and Writing-Original Draft Preparation. **Sumardi Hadi Sumarlan**: Project Administration, Validation, Supervision, and Funding Acquisition. **Hammam**: Software, Investigation, and Writing- Reviewing.

Declaration of Competing Interest

I have no declare under financial, general, and institutional competing interests

Acknowledgement

Thank you to Brawijaya University for providing funding for this research through the Brawijaya University LPPM Professor Grant Program. Sincere gratitude is also extended to Prof. Dr. Ir. Sandra Malin Sutan, MP, as thesis advisor, for his valuable contributions in the validation

and supervision processes during the preparation of this article.

References

[1] Hussein Z, Fawole OA, Opara UL. Harvest and Postharvest Factors Affecting Bruise Damage of Fresh Fruits. Horticultural Plant Journal 2020;6:1–13. https://doi.org/10.1016/j.hpj.2019.07.006.

[2] Mohan VB, Lau K tak, Hui D, Bhattacharyya D. Graphene-based materials and their composites: A review on production, applications and product limitations. Composites Part B: Engineering 2018;142:200–20. https://doi.org/10.1016/j.compositesb.2018.01.013.

[3] Senthamaraikannan P, Saravanakumar SS, Sanjay MR, Jawaid M, Siengchin S. Physico-chemical and thermal properties of untreated and treated Acacia planifrons bark fibers for composite reinforcement. Materials Letters 2019;240:221–4. https://doi.org/10.1016/j.matlet.2019.01.024.

[4] Arivalagan M, Karunakaran G, Roy TK, Dinsha M, Sindhu BC, Shilpashree VM, et al. Biochemical and nutritional characterization of dragon fruit (Hylocereus species). Food Chemistry 2021;353:129426. https://doi.org/10.1016/j.foodchem.2021.129426.

[5] Jalgaonkar K, Mahawar MK, Bibwe B, Kannaujia P. Postharvest Profile, Processing and Waste Utilization of Dragon Fruit (Hylocereus Spp.): A Review. Food Reviews International 2022;38:733–59. https://doi.org/10.1080/87559129.2020.1742152.

[6] Choudhury AG, Sen J, Chandra B, Barman M, Das S. Technological Advancement for Sustainable Post-harvest Quality and Storage of Dragon Fruit [Hylocereus Species (Haworth) Britton & Rose] 2018. https://www.researchgate.net/publication/328628857

[7] Kerr WL. Food drying and evaporation processing operations. Elsevier Inc.; 2019. https://doi.org/10.1016/B978-0-12-814803-7.00014-2.

[8] Shafigh P, Asadi I, Mahyuddin NB. Concrete as a thermal mass material for building applications - A review. Journal of Building Engineering 2018;19:14–25. https://doi.org/10.1016/j.jobe.2018.04.021.

[9] Animasaun IL, Shah NA, Wakif A, Mahanthesh B, Sivaraj R, Koriko OK. Ratio of Momentum Diffusivity to Thermal Diffusivity: Introduction, Meta-Analysis, and Scrutinization. Boca Raton: CRC Press; 2022.

[10] Hutabarat MA, Hasbullah R, Solahudin M. Perlakuan Uap Panas dan Pengaruhnya Terhadap Mutu Buah Melon (Cucumis melo L.) Selama Penyimpanan. Jurnal Teknik Pertanian Lampung 2019;8. http://dx.doi.org/10.23960/jtep-l.v8i2.65-75

[11] Mohsenin NN. Thermal Properties of Food and Agricultural Materials. Boca Raton: CRC Press; 2020.

[12] Hawa LC, Sugesti A, Wibisono Y, Mardiyani SA. Penentuan Sifat Termal Cabai Puyang (Piper retrofractum Vahl.) Kering Pada Tiga Tahap Kematangan. Agrointek : Jurnal Teknologi Industri Pertanian 2022;16:123–33. https://doi.org/10.21107/agrointek.v16i1.8996.

[13] Nurullaeli AMN, Nugraha AM. Media Bantu Simulasi Distribusi Panas Pada Batang 2021:837–41. https://proceeding.unindra.ac.id/index.php/semnasristek/article/viewFile/5075/913.

[14] Emmilia M. Simulasi Perubahan Suhu dalam Buah Alpukat (Persea americana Mill) Pada Proses Pendinginan. [Thesis]: Malang: Fakultas Teknologi Pertanian, Universitas Brawijaya; 2007.

[15] Noor I, Fitrian A, Huda DN. Prosiding Seminar Nasional Sains Simulasi Distribusi Temperatur pada Pelat Tipis Berbantuan FDM (Finite Difference Method) 2020;1:1–5. https://proceeding.unindra.ac.id/index.php/sinasis/article/.

[16] SNI. Cara uji makanan dan minuman 1992:23. https://www.slideshare.net/slideshow/sni-01-28911992-cara-uji-makanan-minuman/16107575.

[17] Nugraheni B, Sulistyowati E. Analisis kimia, makronutrien dan kadar glukomanan pada

tepung umbi porang (Amorphalus konjac K. Koch.) setelah dihilangkan kalsium okslatnya menggunakan NaCl 10%. Repository STIFAR 2018:92–101. https://repository.stifar.ac.id/Repository/article/view/46/73

[18] Saraswati LD, Arifan F, Muhammad F, Yuliana RAD, Nissa C. Nutrition assessment of "kamir"-typical food of pemalang, Central Java Province, Indonesia. Journal of Physics: Conference Series 2019;1217. https://doi.org/10.1088/1742-6596/1217/1/012047.

[19] Subroto E, Lembong E, Filianty F, Indiarto R, Primalia G, Putri MS, et al. The Analysis Techniques Of Amino Acid And Protein In Food And Agricultural Products. International Journal of Scientific & Technology Research 2020;9:29–36. https://www.ijstr.org/final-print/oct2020/The-Analysis-Techniques-Of-Amino-Acid-And-Protein-In-Food-And-Agricultural-Products.pdf.

[20] Jamal S, Jamil D, Khidhir Z. Protein Determination in some Animal Products from Sulaymaniyah Markets Using Kjeldahl Procedure. Journal of Food and Dairy Sciences 2020;11:343–6. https://doi.org/10.21608/jfds.2020.160394.

[21] Bilge G, Sezer B, Eseller KE, Berberoglu H, Koksel H, Boyaci IH. Ash analysis of flour sample by using laser-induced breakdown spectroscopy. Spectrochimica Acta - Part B Atomic Spectroscopy 2016;124:74–8. https://doi.org/10.1016/j.sab.2016.08.023.

[22] Agustina R, Syah H, Moulana R. Karakteristik Pengeringan Biji Kopi dengan Pengering Tipe Bak dengan Sumber Panas Tungku Sekam Kopi dan Kolektor Surya. Jurnal Ilmiah Teknologi Pertanian AGROTECHNO 2016;1:20–7. https://ojs.unud.ac.id/index.php/agrotechno/article/view/22016/14599

[23] Senin SF, Hamid R. Ground penetrating radar wave attenuation models for estimation of moisture and chloride content in concrete slab. Construction and Building Materials 2016;106:659–69. https://doi.org/10.1016/j.conbuildmat.2015.12.156.

[24] BPOM. Pedoman Evaluasi Mutu Gizi dan Non Gizi Pangan 2019. https://standarpangan.pom.go.id/dokumen/pedoman/Pedoman-Evaluasi-Mutu-Gizi-dan-Non-Gizi-Pangan.pdf

[25] Kanzler S, Manschein M, Lammer G, Wagner KH. The nutrient composition of European ready meals: Protein, fat, total carbohydrates and energy. Food Chemistry 2015;172:190–6. https://doi.org/10.1016/j.foodchem.2014.09.075.

[26] Sahubawa L, Pratomo SA. Nutritional Composition and Consumer Preference Level from Hanpen Fish Cake Based on African Catfish Surimi and Cassava Flour. IOP Conference Series: Earth and Environmental Science 2022;1118. https://doi.org/10.1088/1755-1315/1118/1/012072.

[27] Mardiyani SA, Sumarlan SH, Argo BD, Laksono AS. Determination of physical and thermophysical characteristics of red peppers (Capsicum annum) using unsteady-state method. AIP Conference Proceedings 2018;1977. https://doi.org/10.1063/1.5042924.

[28] Macedo LL, Corrêa JLG, Araújo C da S, Vimercati WC, Pio LAS. Process optimization and ethanol use for obtaining white and red dragon fruit powder by foam mat drying. Journal of Food Science 2021;86:426–33. https://doi.org/10.1111/1750-3841.15585.

[29] Singh RP, Heldman DR. Introduction to food engineering: Fifth edition. 2014. https://doi.org/10.1016/C2011-0-06101-X.

[30] Owczarek M. Parametric study of the method for determining the thermal diffusivity of building walls by measuring the temperature profile. Energy and Buildings 2019;203. https://doi.org/10.1016/j.enbuild.2019.109426.

[31] Song N, Cao D, Luo X, Wang Q, Ding P, Shi L. Highly thermally conductive polypropylene/graphene composites for thermal management. Composites Part A: Applied Science and Manufacturing 2020;135:105912. https://doi.org/10.1016/j.compositesa.2020.105912.

[32] Uetani K, Hatori K. Thermal conductivity analysis and applications of nanocellulose materials. Science and Technology of Advanced Materials 2017;18:877–92. https://doi.org/10.1080/14686996.2017.1390692.

[33] Abdullah SA. Nutritional Value and Quality Standard of Popcorn Cooked by Microwave and Conventional Heating. IOP Conference Series: Earth and Environmental Science 2021;910. https://doi.org/10.1088/1755-1315/910/1/012035.
[34] Holman JP. Perpindahan Kalor (Heat Transfer). Jakarta: Penerbit Erlangga; 1984.
[35] Rofi'ah S. Studi Penetapan Sifat Termal Berbagai Varietas dan Konsentrasi Puree Buah Naga (Hylocereus sp.). [Thesis]: Jember: Fakultas Teknologi Pertanian, Universitas Jember; 2013.
[36] Bhagya Raj GVS, Dash KK. Heat transfer analysis of convective and microwave drying of dragon fruit. Journal of Food Process Engineering 2021;44:1–14. https://doi.org/10.1111/jfpe.13775.
[37] Karneta R, Rejo A, Priyanto G, Pambayun R. Penentuan Difusivitas Panas Pempek Lenjer Selama Perebusan Menggunakan Metode Numerik. Jurnal Agritech 2015;35:18. https://doi.org/10.22146/agritech.9415.
[38] Kumar C, Millar GJ, Karim MA. Effective Diffusivity and Evaporative Cooling in Convective Drying of Food Material. Drying Technology 2015;33:227–37. https://doi.org/10.1080/07373937.2014.947512.
[39] Sutarsi S, Taruna I, Hanun J. Effect of Cooling on Thermal Properties of Tomato (Solanum Lycopersicum). UNEJ E-Proceeding 2022:10–21. https://jurnal.unej.ac.id/index.php/prosiding/article/view/32158%0A.
[40] Zain NF, Pantjajani T, Askitosari TD. Studi Literatur: Aplikasi dan Fungsi Porang (Amorphophallus Oncophyllus) dalam Frozen Yoghurt. KELUWIH: Jurnal Sains Dan Teknologi 2021;2:70–80. https://doi.org/10.24123/saintek.v2i2.4635.
[41] Phinney DM, Frelka JC, Heldman DR. Composition-Based Prediction of Temperature-Dependent Thermophysical Food Properties: Reevaluating Component Groups and Prediction Models. Journal of Food Science 2017;82:6–15. https://doi.org/10.1111/1750-3841.13564.
[42] Hung Anh LD, Pásztory Z. An overview of factors influencing thermal conductivity of building insulation materials. Journal of Building Engineering 2021;44. https://doi.org/10.1016/j.jobe.2021.102604.
[43] Sulistyaningtyas AD, Wantika RR. Profil Distribusi Panas Menggunakan Skema Beda Hingga dengan Pengaruh Variasi Nilai Sumbu Mayor. Journals of Mathematics and Mathematics Education 2022;7:108–16. https://doi.org/10.26594/jmpm.v7i2.2923.